Experimental Study of the Behaviour of a New Replaceable Bracing System (BBBS)

S.V. Khonsari, M. Moradi, D. Zarei & H. Farahani
Sharif University of Technology, Iran

G.L. England
Imperial College London, U.K.

SUMMARY:
A new bracing system with new features somewhat different from those of the existing ones was devised and is presented. These features comprise some of the advantages of eccentric bracing systems including their ability to dissipate energy through bending of flexural elements while lacking some of the disadvantages of such systems including their inability of being replaced upon damage during events such as earthquakes, etc. While in traditional types of braces, including both concentric and eccentric ones, braces are under axial loading, in this new system they work in a bending capacity. As a result, the sort of flexibility which is introduced in the system in the presence of eccentric braces (definitely at the price of forcing the potential damage to occur and be concentrated at the girders/beams to which such braces are connected), is now provided by the braces and at the price of sacrificing them. Therefore, if the level of damage is such that the damaged element is no longer usable, the replacement of the braces is a more viable and economically justifiable than that of the girders. Moreover, since girders, as part of the deck/floor system, are normally engaged with other elements such as stringers/joists, their replacement may not be practically possible at all. Such bracing systems, called Broken Beam Bracing System (BBBS), have the potential of being used in building as well as industrial structures as originally-used elements or in a retrofit/repair capacity.

Keywords: Structural Bracing Systems, Replaceable Bracings, Cyclic Loading, Energy Dissipation, Retrofitting

1. INTRODUCTION

As efficient elements for controlling the deflections of structures against various lateral loads, braces have a long history of service. While initially they were used to resist wind, they gradually found their way into the seismic design of structures as efficient means of controlling the lateral drift. Here they regulate the performance of the structure under dynamic cyclic earthquake induced forces. So far, braced frames have been divided into two major categories, viz. Concentrically-Braced Frames (CBFs) and Eccentrically-Braced Frames (EBFs)—the former have high elastic stiffness and more rigid behaviour hence react poorly to cyclic loading. The latter have more flexible nature and good response to such loading (Bruneau, *et al.,* 1998). EBFs which have become popular during the past two decades have the disadvantage of using the beam (to which the braces are connected) in a *sacrificial capacity.* Therefore, if the level of incurred damage is so high that it requires replacement, due to the engagement of the beam with the floor system (slab, joists/stringers) such replacement is basically neither technically viable nor economically justifiable. Taking advantage of the concept of EBFs, a geometrically similar, but different in nature, system has been developed which seems to have the advantages of eccentric braces and lack their major disadvantage, *viz. irreplaceability.* Similar to eccentric braces and unlike concentric ones, they add to the weight of the structure, but what one receives is an improved performance under cyclic loading with better-shaped hysteresis loops, as demonstrated through limited number of test described in this paper.

2. DESCRIPTION OF THE BROKEN BEAM BRACING SYSTEM (BBBS)

Developed by the first author, the new bracing system comprises two bending-axial (beam-column) elements connected to one another through a semi-rigid joint. It resembles stair framing—in fact stair framing systems work in the same capacity. Figure 1(a) depicts a portal frame with hinge joints equipped with such system. Apparently, in such a case a minimum rigidity for the joint between the two pieces of the bracing system is required in order to maintain the stability of the frame and also limit its drift to the permissible amount required by the code. Figure 1(b) shows the detail of the semi-rigid connection between the two segments of the brace. In this Figure it has been attempted to show the fact that there is not (indeed should not be) any interaction between the beam and the horizontal segment of the brace. Moreover, the semi-rigid behaviour of the connection between the two segments of the brace is emphasized. Figure 1(c) reveals the *'two-force'* nature of the brace which emanates solely from relative overall displacements of the two ends of the brace; there being no other loading.

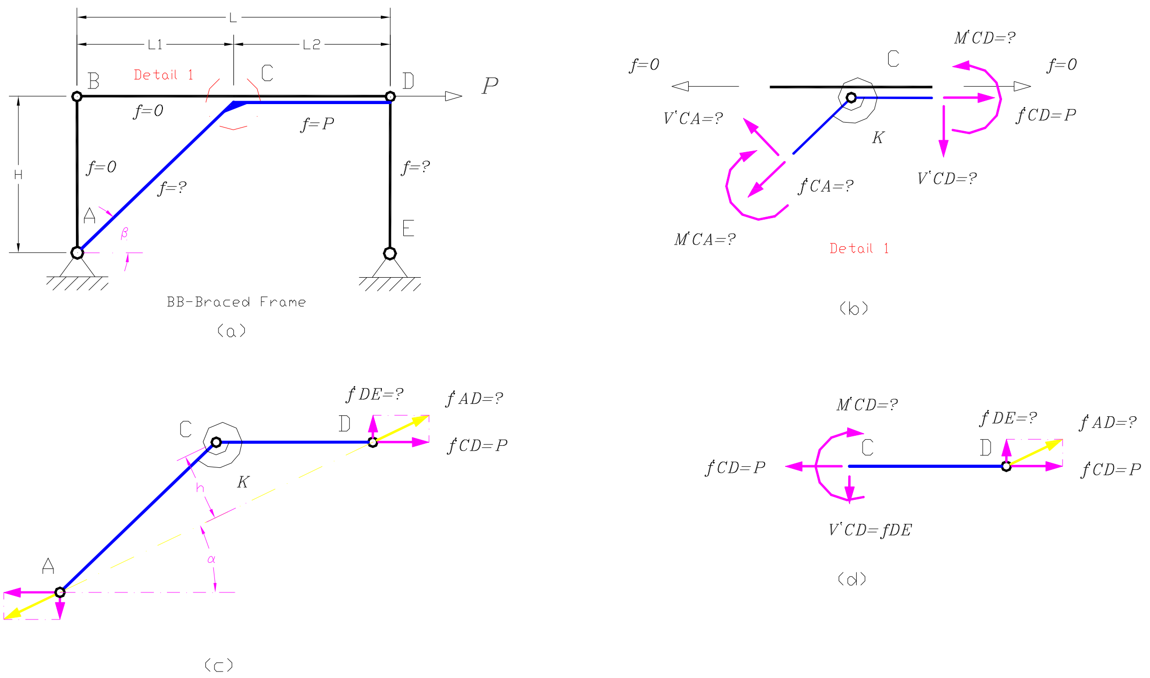

Figure 1. The Broken Beam Bracing System (BBBS) and its geometric and mechanical details. (a) The brace, shown in blue, fitted into a portal frame; (b) Detail 1 and the lack of physical contact between the beam and the brace; (c) the free-body diagram of the brace and the largest moment arm (*h*) which leads to the maximum bending moment occurring at the brace knee; (d) free-body diagram of the horizontal segment of the brace.

The following simple statics calculations show that

$$f_{AD} = \frac{f_{CD}}{\cos\alpha} = \frac{P}{\cos\alpha} \tag{2.1}$$

$$f_{DE} = f_{AD}.\sin\alpha = \frac{P}{\cos\alpha}.\sin\alpha = P.\tan\alpha = P.\frac{H}{L} \tag{2.2}$$

As it is shown in Fig. 1(c), since the maximum distance between various points on the brace and the line connecting its two ends occurs at C and is equal to h, therefore, the maximum bending moment occurs at C,

$$M_{\max} = M_C = f_{DE}.L_2 = P.\frac{H}{L}.(L - L_1) = P.\frac{H}{L}.\left(L - \frac{H}{\tan\beta}\right). \tag{2.3}$$

Here, it can be easily seen that the bending moment is a minimum when $\tan\beta$ is a minimum, i.e. when the horizontal segment of the brace diminishes and the brace turns into a straight member and works in an axial capacity, or

$$\beta \to \alpha \, . \tag{2.4}$$

In other words, when it becomes a traditional *'Concentric Diagonal Bracing'* with no moment developing in it. And, this is very well in line with 'common sense.' On the other hand, bending moment becomes a maximum when is a maximum, i.e. when

$$\beta \to \pi / 2 \, . \tag{2.5}$$

In other words, when the two segments of the brace are normal to one another and in fact it turns the fame into a *'Moment-Resisting Frame.'* Therefore, it is not false if we say that this bracing system, BBBS, works in such a capacity that turns the frame into something between a Concentrically-Braced Frame (CBF) and a Moment-Resisting Frame (MRF). As a result, it should be expected to see some features of the two systems being combined in this system. However, comparing with EBF systems (despite their positive features which have recently made them popular), where damage is incurred in the main beam to which the braces are attached BBBS should provide considerable benefits.

3. EXPERIMENTAL PROGRAMME

To assess the performance of the system an experimental programme was conducted. Since it is in a cyclic loading context that the performance of the new bracing system is intended to be exploited it would be meaningful to carry out the tests under cyclic loading. However, since this type of bracing has not been used in the past, there seemed to be no specifications for testing them. Therefore, (due to the similarity which exists between the bending behaviour of this system and that of the links of EBFs), it was decided to use the instructions given by AISC (2005) for testing *Link-to-Column Connections*. Based on these instructions, the total link rotation angle, γ, is specified on a cycle by cycle basis. The corresponding loads are then monitored. Details of the recommended rotations for each cycle of testing are given in Table 1. The test facility shown schematically in Fig. 2 was used to test three braces of different section dimensions, *viz.* IPE100, HE-A100, and 2UNP100. These are standard beam, light column and channel sections, respectively, based on DIN-1025 or EURONORM-53-62 standards.

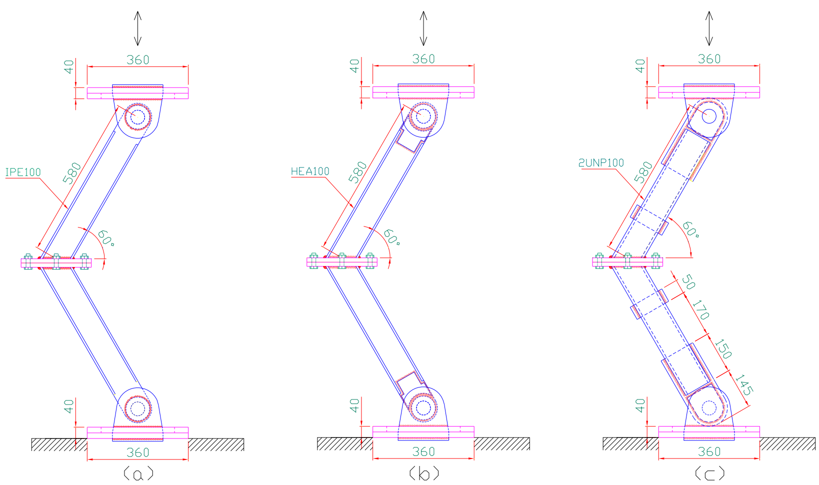

Figure 2. The test assemblies designed and fabricated to enable the authors to apply cyclic loading to the specimens of the bracing system. Brace segments were fabricated from (a) IPE100, (b) HE-A100, and (c) 2UNP100 sections.

In order to convert the rotation angles γ, given by AISC (2005), to linear displacements of the loading equipment (machine), Δ, (Fig. 3), the following approximate formulae were used,

$$\Delta 1 = 2L.\cos(30 - \gamma / 2) - 2L.\cos 30 \quad (3.1)$$

$$\Delta 2 = 2L.\cos 30 - 2L.\cos(30 + \gamma / 2) \quad (3.2)$$

$$L = 580 \text{ mm} . \quad (3.3)$$

Approximate, in this sense that a hinge connection is assumed to form at the joint between the two segments. Due to the differences between the geometries of the two situations, (tensile and compressive), the tensile and compressive deformations (deformation amplitudes) are different and this difference increases as the angle of rotation increases (see Table 1).

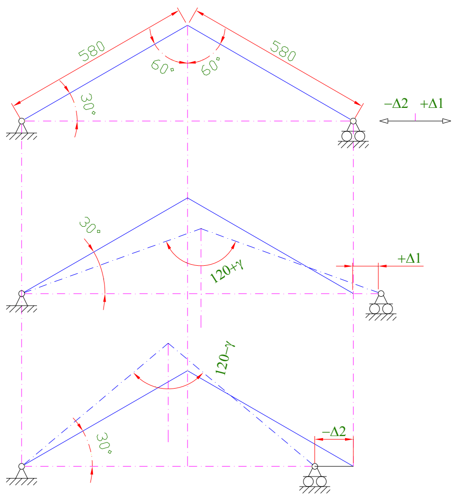

Figure 3. The idealized model of the bracing system subjected to linear displacements in tension (Δ1) and compression (Δ2) to create the rotation angles prescribed by AISC (2005) between the two segments.

Table 1. The amplitudes of displacement cycles in tension and compression worked out based on the instructions given by AISC (2005) for the rotation of the links of EBFs and the simple model of Fig. 3, together with the number of cycles of each stage.

Stage	No. of Cycles	Rotation Angle γ (radian)	Tensile Amplitude Δ1 (mm)	Compressive Amplitude Δ2 (mm)
1	6	0.00375	1.0857	1.0893
2	6	0.005	1.4469	1.4531
3	6	0.0075	2.1679	2.1821
4	6	0.01	2.8874	2.9125
5	4	0.015	4.3217	4.3782
6	4	0.02	5.7497	5.8501
7	2	0.03	8.5867	8.8127
8	1	0.04	11.3983	11.8001
9	1	0.05	14.1846	14.8124
10	1	0.07	19.6806	20.9111
11	1	0.09	25.0742	27.1082
12	1	0.11	30.3649	33.4030
13	1	0.13	35.5520	39.7949
14	1	0.15	40.6351	46.2833
15	1	0.17	45.6138	52.8675
…	1	…	…	…

All the three specimens were subjected to the above loading pattern, each up to a stage where signs of severe destruction were observed. Due to the diversity of the sections of the specimens, different types of response were observed.

3.1. 1st Test: Using IPE100 Section

The section used for the bracing segments, IPE100, is an ordinary I section with small flange width compared to the overall section height. As a result, the ratio of the moments of inertia of the section about its two principal axes is

$$r = \frac{I_{xx}}{I_{yy}} = \frac{171}{15.9} = 10.75\,. \tag{3.4}$$

Therefore, it was anticipated that at some point during the test, signs of lateral buckling could occur. Indeed, as the test proceeded from the 11th stage the specimen started to undergo lateral movement with its maximum at the joint between the two segments of the brace. The effect of this phenomenon was a substantial drop in the compressive test load *(strength degradation).* Towards the end of the 14th stage the extent of lateral deformations increased to a level that was unacceptable to the test apparatus and the test was therefore halted. Figure 4 shows the first specimen before the test, while Figs. 5 shows its side view at the end of the test with the lateral buckling which had already started to emerge at compressive half cycles of earlier stages, now at its most severe state.

Figure 4. The 1st specimen, with IPE100 sections, before the test.

Figure 5. Side view of the 1st specimen at the end of the test with maximum observed out-of-plane displacements.

Although this test was terminated due to pronounced ‘out-of-plane’ buckling, the brace could still be used provided lateral deformations can be restricted. Figure 6 illustrates how this might be achieved, by the provision of additional bracing from adjacent frames. Some extra costs would then be involved, but overall the system could still be economically justifiable.

The hysteresis loops of this test, 1st test, are depicted in Fig. 7.

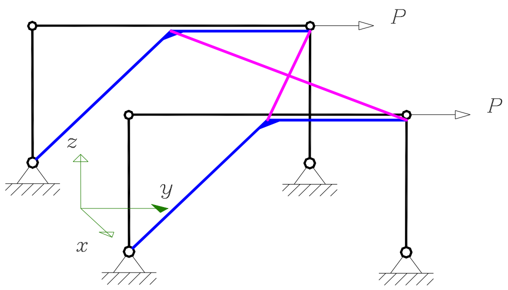

Figure 6. A suggested extra bracing system (in horizontal plane in magenta) to prevent the devised bracing system from having out-of-plane (lateral) deformations (buckling).

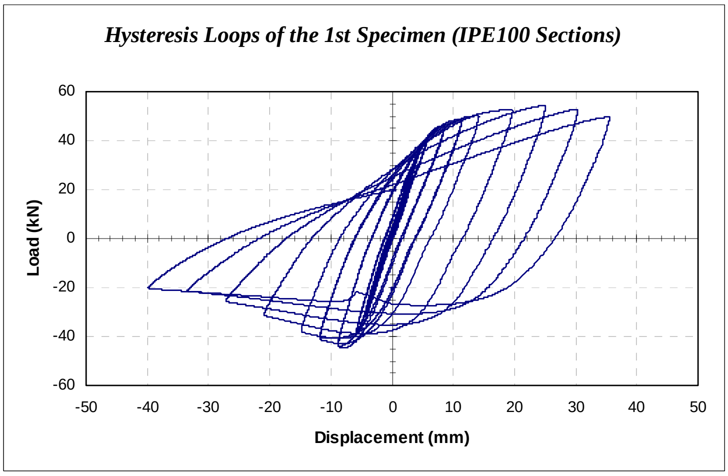

Figure 7. Hysteresis loops of the 1st test assembly with IPE100 sections used for the two segments of the devised Broken Beam Bracing System.

The effect of buckling is clearly apparent in Fig. 7 where the maximum compressive force is much less than the maximum tensile force during the latter cycles of the test.

3.2. 2nd Test: Using HE-A100 Section

HE-A is a light wide flange section compared to HE-B and HE-M which are medium-weight and heavy wide flange sections. The real height of HE-A100 is 96 mm while its flange width is 100 mm. The ratio of the moments of inertia about the two principal axes of this section is

$$r = \frac{I_{xx}}{I_{yy}} = \frac{349}{134} = 2.60 \,. \qquad (3.5)$$

Out-of-plane buckling that was observed in the 1st test should not be observed in this test. Indeed no sign of lateral buckling was observed. Failure of the weld of the bracing to the endplate at the joint between the two segments halted this test. Since the overall geometry of the specimen was the same as that of the previous test, the same amplitudes for the displacements of each stage of loading were used (see Table 1). The much stronger cross section compared with that of the 1st test led to higher levels of resistance (load) being observed. The number of cycles to premature failure of the end plate welds was the same as for Test 1, *viz.* 40 cycles. The specimen's increased stiffness and strength were not therefore completely exploited. Figure 8 shows the specimen before the test, whereas Figs. 9 and 10 depict the weld failure and the crack that developed at the joint between the weld and the endplate. The local buckling which occurred at the lower flange of the upper segment in the vicinity of the endplate is shown in Fig. 11. The hysteresis loops of this test, 2nd test, are depicted in Fig. 12.

Figure 8. The 2nd specimen, with HE-A100 sections, before the test.

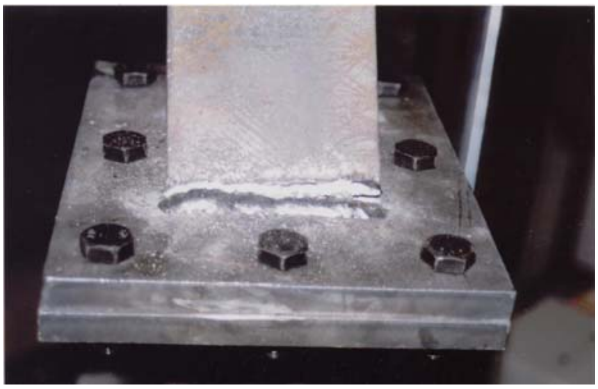

Figure 9. Developed cracks at the joint between the upper segment and its endplate caused by 'lack of fusion.'

Figure 10. Developed cracks at the other side of the upper segment of the 2nd test assembly with HE-A100 sections.

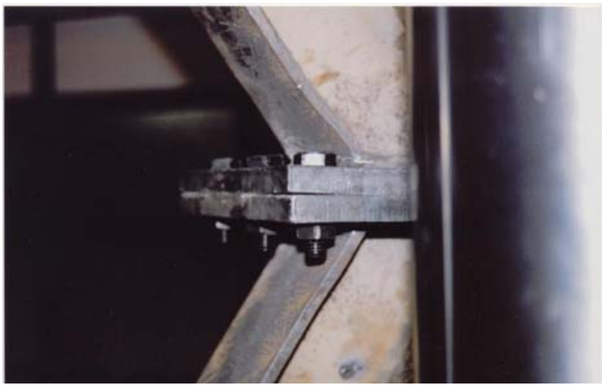

Figure 11. Local buckling of lower flange of the upper segment of the 2nd test assembly with HE-A100 sections.

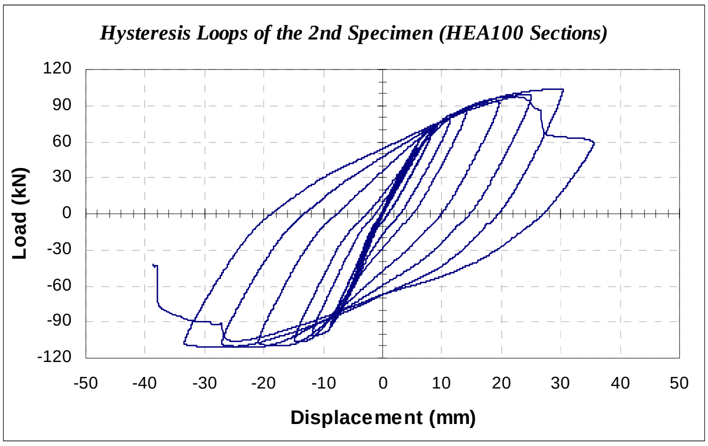

Figure 12. Hysteresis loops of the 2nd test assembly with HE-A100 sections used for the two segments of the devised Broken Beam Bracing System.

3.3. 3rd Test: Using 2UNP100 Sections

As an alternative to the previous sections and in order to investigate the behaviour of a fairly commonly-used section for bracing systems, a double channel section was used. UNP100 is a Normal U Profile with 100 mm height, 50 mm flange width, 6 mm web thickness and 8.5 mm average flange thickness. For this double section (with 10 mm clear distance between their flange edges, see Fig. 13), the ratio of the moments of inertia around principal axes is

$$r = \frac{I_{xx}}{I_{yy}} = \frac{412}{480} = 0.858\,. \tag{3.6}$$

This low ratio precluded any lateral buckling from occurring and the test was terminated when one of the welds between the element ends and the endplate fractured. As in previous tests the same displacement inputs (Table 1) were employed here. The overall front view of the specimen is shown in Fig. 14 while its side view is demonstrated in Fig. 15. The developed crack in the weld of the brace-segment/brace-endplate is shown in Fig. 16. The hysteresis loops of this test, 3rd test, are depicted in Fig. 17. Observation reveals considerably less ductility and less energy dissipation, cycle by cycle, compared to the previous tests. This test was halted in the 36th cycle.

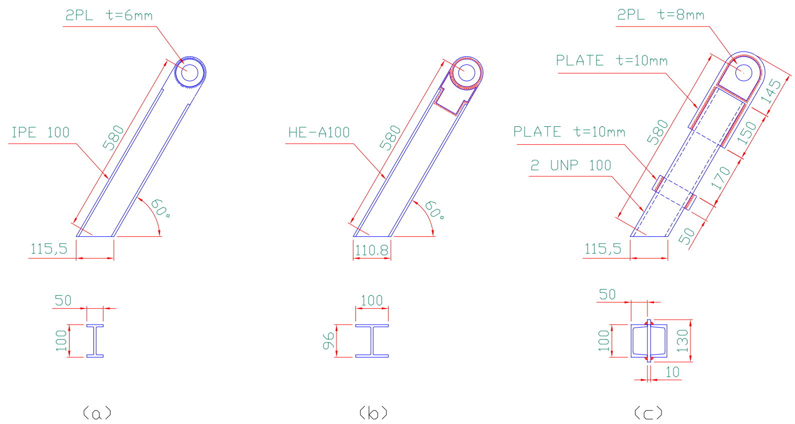

Figure 13. Details of the members of various test assemblies and their cross sections.

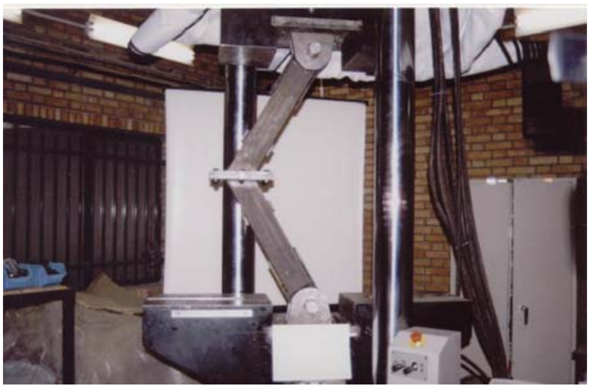

Figure 14. Overall front view of the 3rd specimens with 2UNP100 sections attached together with 10 mm thick battens.

Figure 15. (Rotated) side view of the 3rd test assembly with 2UNP100 sections attached together with 10 mm batten plates—one at the middle of each segment and one being the eye-bar of the hinge connection at one end of each segment.

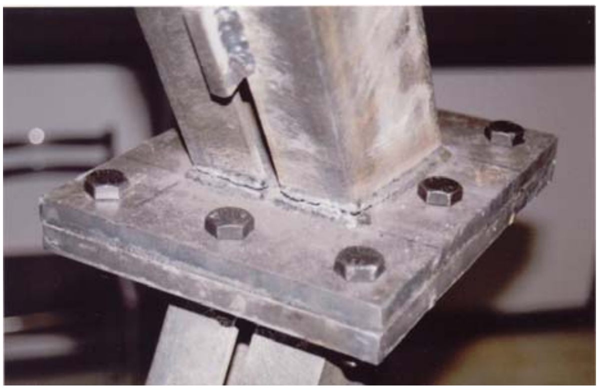

Figure 16. The developed cracks and the detachment of the upper segment and its endplate due to 'lack of fusion.'

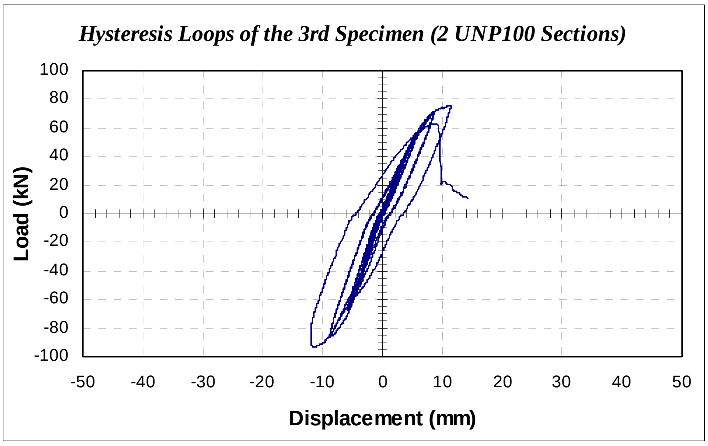

Figure 17. Hysteresis loops of the 3rd test assembly with 2UNP100 sections used for the two segments of the devised Broken Beam Bracing System.

4. DISCUSSION

In order to have a proper judgment on the performance of this system, the total cumulative dissipated energy for each test is worked out. This figure together with the values of maximum load and displacement endured by each specimen (in tension and compression) are shown in Table 2 for the 1st, 2nd and 3rd specimens, respectively. Moreover, for each specimen, number of stages and also the number of cycles of loading endured by each specimen are shown in this Table. These results provide the reader with useful information to make comparisons between the different test specimens. Although only three tests were carried out on the specimens of this type of bracing system, each was beneficial in revealing some facts about its performance. The first test was beneficial in that it showed the vulnerability of sections with low minor-axis stiffness to lateral buckling. However, despite severe out-of-plane deformations the amount of energy dissipated in each cycle of loading gradually increased as the amount of stroke increased, eventually reaching an appreciable value. This is an indication of the effectiveness of the slender elements to deform appreciably during every cycle. The use of stiffer sections led to improvements in the cyclic behaviour of the system and dissipated more energy than the specimen of test 1, as far as the fifth loading stage and again after stage 11 when lateral buckling was observed in test 1. Due to the premature failure of the end plate welds in test 2 the final capacity of the section for the dissipation of energy was not realized. As far as the authors are concerned, the *lack of fusion phenomenon,* about which many welding experts have already warned (Salmon and Johnson, 1980), was the main cause of failure for the 2nd and 3rd specimens. With a standard welding practice, this should be easily solved. Regarding the 3rd specimen, this phenomenon existed in a much more pronounced manner, hence causing the termination of the test at an earlier stage compared with the 2nd test. Without these premature failures these two specimens were expected to show much higher efficiency in absorbing and dissipating energy under cyclic loading and therefore be suitable for use as braces in buildings or installations built and used in environments prone to experiencing cyclic loadings such as wave or earthquake. All of the tests suffered to some extent from premature weld failures which prevented the full plastic moment capacity of the element sections from being realized.

Table 2. Overall performance of various tested specimens.

Specimen (Brace Sections)	No. of Stages of Loading Endured	No. of Cycles Endured	Max. Tensile Diametral Displacement (mm)	Max. Compressive Diametral Displacement (mm)	Max. Tensile Diametral Load (kN)	Max. Compressive Diametral Load (kN)	Total Cumulative Dissipated Energy (J)
IPE100	14	42*	35.57	-39.82	52.89	-46.00	13206.83
HE-A100	13	40*	35.56	-38.58	104.03	-111.14	22083.05
2UNP100	9	36*	14.18	-11.82	75.56	-93.15	2538.23

*) The last cycle was an incomplete cycle.

5. CONCLUSIONS

Using the limited tests reported in this paper, the following conclusions, with some degree of caution, can be drawn.

1- The hysteresis loops of the specimens have demonstrated the suitability of the devised bracing system, BBBS, for energy dissipation under cyclic loading.

2- As in other types of bracing system, more traditional concentric and more modern eccentric ones, the role of the shape of the cross section is quite important. Using sections with large difference in their moments of inertia about their two principal axes makes the system susceptible to lateral buckling if the angle between the two segments of the brace is fairly large and to in-plane buckling if the angle is small.

3- As in other types of bracing system, the role of connections of the braces to the frame should be considered though in this investigation such effects were not studied.

4- Since the maximum bending moment in the brace occurs at the bent (breaking point), the design and fabrication of the joint between the two segments have a crucial role in the behaviour as well as service life of the system. In this regard the quality of the welds must not be compromised—full fusion welds should be used for these connections and their elements.

ACKNOWLEDGEMENT

Financial and technical support of this project by Sharif University of Technology is gratefully acknowledged.

REFERENCES

AISC (2005). Seismic Provisions for Structural Steel Buildings, American Institute of Steel Construction, Chicago, Ill.

Bruneau, M., Uang, C.M. and Whittaker, A. (1998). Ductile Design of Steel Structures, McGraw-Hill, Boston, Massachusetts.

Salmon, C.G. and Johnson, J.E., 1980, “Steel Structures, Design and Behavior,” 2nd Edition, Harper & Row, Publishers, N.Y.